



UNIVERSITY OF LEEDS

This is a repository copy of *Hierarchical management for integrated community energy systems*.

White Rose Research Online URL for this paper:
<http://eprints.whiterose.ac.uk/144197/>

Version: Accepted Version

Article:

Xu, X, Jin, X, Jia, H et al. (2 more authors) (2015) Hierarchical management for integrated community energy systems. *Applied Energy*, 160. pp. 231-243. ISSN 0306-2619

<https://doi.org/10.1016/j.apenergy.2015.08.134>

Crown Copyright © 2015 Published by Elsevier Ltd. This manuscript version is made available under the Creative Commons CC-BY-NCND 4.0 license
<http://creativecommons.org/licenses/by-nc-nd/4.0/>.

Reuse

This article is distributed under the terms of the Creative Commons Attribution-NonCommercial-NoDerivs (CC BY-NC-ND) licence. This licence only allows you to download this work and share it with others as long as you credit the authors, but you can't change the article in any way or use it commercially. More information and the full terms of the licence here: <https://creativecommons.org/licenses/>

Takedown

If you consider content in White Rose Research Online to be in breach of UK law, please notify us by emailing eprints@whiterose.ac.uk including the URL of the record and the reason for the withdrawal request.



eprints@whiterose.ac.uk
<https://eprints.whiterose.ac.uk/>

1 Hierarchical management for integrated community energy systems

2 **Xiandong Xu^{a*}, Xiaolong Jin^b, Hongjie Jia^b, Xiaodan Yu^b, Kang Li^a**

3 ^a School of Electronics, Electrical Engineering and Computer Science, Queen's University Belfast,
4 Belfast BT9 5 AH, UK

5 ^b Key Laboratory of Smart Grid of Ministry of Education, Tianjin University, Tianjin 30072, China

6 Email address: x.xu@qub.ac.uk, xljin@tju.edu.cn, hjjia@tju.edu.cn, yuxd@tju.edu.cn, k.li@qub.ac.uk

7 **Abstract**

8 Due to the presence of combined heat and power plants (CHP) and thermostatically controlled
9 loads, heat, natural gas and electric power systems are tightly coupled in community areas.
10 However, the coordination among these systems has not been well considered, especially with
11 the integration of renewable energy. This paper aims to develop a hierarchical approach for an
12 integrated community energy system (ICES). The proposed hierarchical framework is presented
13 as day-ahead scheduling and two-layer intra-hour adjustment systems. Two objectives, namely
14 operating cost and tie-line power smoothing, are integrated into the framework. In the intra-hour
15 scheduling, a master-client structure is designed. The CHP and thermostatically controlled loads
16 are coordinated by a method with two different time scales in order to execute the schedule and
17 handle uncertainties from the load demand and the renewable generation. To obtain the optimal
18 set-points for the CHP, an integrated optimal power flow method (IOPF) is developed, which
19 also incorporates three-phase electric power flow and natural gas flow constraints. Furthermore,
20 based on a time priority list method, a three-phase demand response approach is proposed to
21 dispatch HVACs at different phases and locations. Numerical studies confirm that the ICES can
22 be economically operated, and the tie-line power between the ICES and external energy network
23 can be effectively smoothed.

24
25 **Keywords:** Hierarchical management, integrated community energy system (ICES), two-layered
26 scheduling, integrated optimal power flow (IOPF), three-phase demand response

27 **1. Introduction**

28 A tendency as the result of global urbanization is that cities are gaining greater control over
29 their development, economically, politically, and technologically, which enables new levels of
30 intelligence [1]. To seize the opportunities and to build sustainable prosperities, integrated
31 community energy systems (ICES) [2] are attracting more and more attentions in recent years,
32 where heat, gas and electrical energy are becoming tightly coupled. It has been shown that the
33 coordination of various energy conversion processes can play a key role in increasing the
34 intermittent energy penetration level, and economic operation, etc. [3-4]. However, to achieve
35 these targets is still quite challenging. This is mainly due to the uncertainty of renewable energy
36 and complex interactions among different energy systems. Therefore, coordination and
37 management of various energy systems are of significant importance for the integration of
38 renewable energy and developing better energy management system for the ICES.

39 Since multiple energy services are required in a community, the integration of various energy
40 systems has been intensively researched, including combined heat and power plants (CHP) [5],
41 microgrids [6], smart energy systems [7], etc. In [8], a general model was presented for a
42 community-based microgrid, integrating renewable generations and CHP plants. A combined
43 analysis was proposed for heat and electricity flow dispatch in a small scale energy system with
44 CHP units [9]. Based on the energy hub (EHub) [10] that was first developed for interrelated
45 energy system description, an integrated optimal energy flow was proposed for multi-carrier
46 energy network optimization in an island [11]. Furthermore, multiple objective were
47 incorporated into the community energy system optimization due to various requirements [12].
48 In addition to the energy supply system, it was shown that utilities and system operators could
49 integrate loads into both decentralized and centralized energy management systems [13-14] and
50 demand response (DR) could be used to reduce the energy consumption and green-house gas
51 emissions. In [15], a two-stage DR scheduling was proposed to integrate renewable energy into
52 power systems. Furthermore, the energy market was integrated into the day-ahead and hourly
53 scheduling system to exchange the DR with variable renewable generation [16].

54 To implement an integrated management of different resources, distributed generations and
55 the DR should be coordinated in the energy management system [17]. It has been shown that
56 the operating cost can be significantly reduced by integrating CHP with the DR in real time
57 control [18]. However, different response characteristics of the CHP and the DR are not well
58 considered in previous studies. Moreover, community energy systems are generally accessed to
59 the low voltage distribution network, which is usually a unbalanced three-phase system [19].
60 However, previous studies usually assume that the community system is balanced. Few
61 discussions have been given to how to manage the loads and generations in three phases.

62 The hierarchical framework offers a measure to handle various objectives and manage the
63 whole system [20]. In [21], a two-level hierarchical framework was presented to handle the
64 uncertainty and to realize an economic generation schedule of microgrids by coordinating
65 battery energy storage systems and distributed generations (DGs). A hierarchical energy
66 management system was proposed in [22] for a multi-source multi-product microgrid with
67 thermal and electrical power storage systems. A multi-agent based hierarchical energy
68 management strategy was implemented by the combination of the autonomous control of
69 distributed energy resources at the local level with the coordinated energy control at the central
70 level of the microgrid [23]. The DR was integrated into the microgrid management system by
71 hierarchical agents [24]. Inspired by the hierarchical framework, this paper aims to develop a
72 novel coordination and management system for the ICES. Firstly, combined with traditional
73 day-ahead scheduling system, a master-client structure is integrated into the hourly adjustment
74 system. The CHP and the DR are dispatched in two time scales in order to handle the long term
75 and short-term forecast errors. Then an integrated optimal power flow (IOPF) algorithm is
76 developed for multiple energy system dispatch considering three-phase electric power flow and
77 gas flow constraints. Two objectives, operating cost and tie-line power smoothing, are integrated
78 into the hierarchical framework for day-ahead scheduling and intra-hour adjustments.
79 Furthermore, a traditional time priority list method is extended to a three phase DR approach in
80 order to utilize the loads in different phases and locations. Numerical tests are performed on a
81 community energy system obtained from a modified IEEE-37 node system. Experimental
82 results demonstrate that the proposed hierarchical framework is effective in interrelated energy

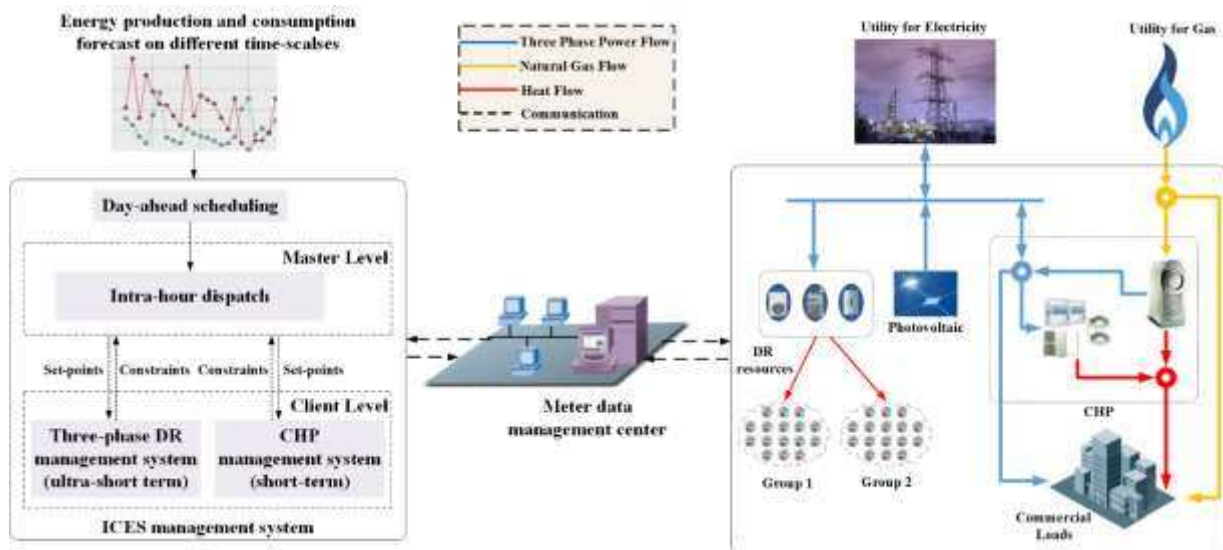
83 system management. The methods and algorithms developed in this paper make it possible to
 84 utilize loads and DGs in three-phase electric power systems.

85 The rest of this paper is organized as follows: Section 2 presents an overview of the
 86 community energy system and the proposed hierarchical energy management system. Section 3
 87 presents a detailed description of the hierarchical framework integrating optimal energy flow
 88 and three-phase DR methodology. Section 4 discusses the results for energy cost reduction,
 89 three-phase scheduling, and tie-line power smoothing. Finally, conclusions and
 90 recommendations are given in Section 5.

91 2. Problem description

92 2.1. Community configuration and energy service provider

93 Community energy systems can have diverse topologies. In this paper, the community model
 94 consists of energy service providers and customers. As shown in Fig. 1, buildings and residential
 95 houses are featured as customers. In buildings, the energy service provider obtains electricity and
 96 gas from utilities and supplies both electricity and heat to customers. In residential houses, the
 97 electricity is supplied to satisfy both heat and electricity demands of customers with
 98 thermostatically controlled loads such as heat pumps, air-conditioners, and heating, ventilating,
 99 and air conditioning (HVAC) units.



100

101

Fig. 1 Framework of the ICES management system

102 The energy service providers own DGs including the CHP and photovoltaic (PV) panels. In
103 real applications, there may be several possible energy service providers. Three of them are
104 listed as follows: (1) Customer owned community energy system. This type of customers own
105 both loads and DGs. The energy supplier only buys energy from utilities without charging the
106 energy users. Also, there is no charge for the DR. The objective can be set to be operating cost
107 minimization; (2) Local energy service retailers owned by third parties. They buy energy from
108 utility and sell energy to customers. The objective is to maximize their profits; and (3) Energy
109 service provided by utilities. This type of energy providers supply energy directly to customers.
110 The objective is to minimize the loss or some other utility requirements.

111 2.2. Integrated optimal power flow (IOPF)

112 As illustrated in Fig. 1, a hierarchical framework is designed to satisfy various requirements
113 of the energy service provider. With load and renewable generation forecast results, day-ahead
114 scheduling results are obtained by calling the IOPF program. The intra-hour scheduling system
115 is further decomposed into a two-layer structure to balance time-varying energy demand and
116 supply forecast errors in two time scales while meet the requirement of interrelated constraints
117 between multiple energy systems. At the master level, the IOPF is called to generate set-points
118 for CHP systems and DR to track load and generation forecast mismatch in both short term and
119 ultra-short term. At the client level, CHP power exchange boundary and the three-phase DR
120 operating constraints are calculated and sent to the master.

121 3. Hierarchical management for the integrated community energy systems

122 3.1. Integrated optimal power flow (IOPF)

123 To optimize the interrelated thermal, gas, and electric power systems, an IOPF program is
124 developed for the ICES. As previously mentioned, economic interests are considered as
125 objectives of energy service providers. In addition, the impacts of renewable integration on the
126 external power grid are also taken into account. For type (1) and (2) energy service providers,
127 they can negotiate with utilities to obtain subsidies by reducing tie-line power fluctuation. For

128 type (3), smoothing tie-line power is one of the utility requirements. Therefore, different
 129 objectives are considered for the two-layered optimization problem to ensure the economic
 130 operation and mitigate adverse impacts of renewable energy sources fluctuations on the power
 131 quality of the external power grid. The clients in this study consist of CHP systems and DR
 132 resources. Considering the diversity of the response time and the capacity of different system
 133 components, different scheduling intervals are set for the CHP systems and the DR resources
 134 respectively in day-ahead scheduling level. Since the CHP systems are not suitable for frequent
 135 adjustment, while DR resources have small regulation range, therefore the CHP systems are
 136 used to match the difference between the load and generation forecast results within a short
 137 control interval, and the DR resources are used to balance the mismatch between the load and
 138 generation forecast results in a ultra-short control interval for guaranting the customer comfort
 139 level.

140 3.1.1. Objectives

141 1) IOPF for day-ahead scheduling

142 To minimize the operating cost, the IOPF program is called to generate set-points for clients.
 143 The control objective is set as follow

$$144 \min \left[P_{e,tl}(k) \frac{\mu_{e,buy}(k) + \mu_{e,sell}(k)}{2} + P_{e,tl}(k) \frac{|\mu_{e,buy}(k) - \mu_{e,sell}(k)|}{2} + \mu_g(k) P_{g,tl}(k) \right] \quad (1)$$

145 where $P_{g,tl}(k)$ is the gas tie-line power, $P_{e,tl}(k)$ is the real electric tie-line power, $\mu_{e,buy}(k)$ and
 146 $\mu_{e,sell}(k)$ represent the electricity prices to purchase and sell respectively at the kth hour, $\mu_g(k)$
 147 represents the gas price at the kth hour. It should be noted that in this paper, DR is only used for
 148 short-period mismatch correction and the cost for DR is not considered and can be a future work.

149 2) IOPF for intra-hour dispatch

150 The ICES is connected to the external power grid and gas network, as shown in Fig. 1. In the
 151 master level, the IOPF program is called to follow the electric and gas tie-line power set-points.
 152 The objective can be formulated as

$$153 \quad \min \left\{ \omega_e \left[P_{e,tl}(k) - P_{e,tl}^{set}(k) \right]^2 + \omega_g \left[P_{g,tl}(k) - P_{g,tl}^{set}(k) \right]^2 \right\} \quad (2)$$

154 where $P_{e,tl}^{set}(k)$ and $P_{g,tl}^{set}(k)$ are set-points of the electric and gas tie-line power at the k th hour.
 155 ω_e and ω_g are weighting factors for electric/gas tie-line power tracking, and when $\omega_g=0$, the
 156 IOPF program is called to follow only the electric tie-line power set-points.

157 3.1.2. Constraints

158 1) Energy network constraints

159 The energy network constraints include three phase electric power flow Eq. (3) [25], and gas
 160 flow Eq. (4) [26] and feasibility domain for control variables Eq. (5)-(7).

$$161 \quad \mathbf{f}_e(\mathbf{P}, \mathbf{Q}, \mathbf{V}, \boldsymbol{\theta}) = 0 \quad (3)$$

$$162 \quad \mathbf{f}_g(\mathbf{M}, \mathbf{p}, \mathbf{k}_{cp}) = 0 \quad (4)$$

$$163 \quad \begin{cases} V_{\min} \leq V_i^a \leq V_{\max} \\ V_{\min} \leq V_i^b \leq V_{\max} \\ V_{\min} \leq V_i^c \leq V_{\max} \end{cases} \quad (5)$$

$$164 \quad p_{\min} \leq p_j \leq p_{\max} \quad (6)$$

$$165 \quad k_{cp,j_c}^{\min} \leq k_{cp,j_c} \leq k_{cp,j_c}^{\max} \quad (7)$$

166 where \mathbf{P} , \mathbf{Q} represent power at the electric node; \mathbf{V} , $\boldsymbol{\theta}$ represent electric node voltage; V_i^a , V_i^b ,
 167 V_i^c represent three-phase voltage at bus i ; V_{\min} and V_{\max} represent lower and upper bounds of
 168 bus voltage; \mathbf{M} represents gas flow; \mathbf{p} is the gas node pressure; \mathbf{k}_{cp} is the compressor ratios;
 169 p_{\min} and p_{\max} represent the lower and upper bounds of gas pressure; k_{cp,j_c}^{\min} and k_{cp,j_c}^{\max} are the
 170 lower and upper bounds of the ratio of compressor j_c .

171 2) CHP constraints

172 The clients in this study include the CHP systems and DR resources. To minimize the
 173 customer discomfort, CHP system is used first to balance the mismatch between the day-ahead
 174 scheduling and the load forecast results in a short control interval. The feasibility domain of the

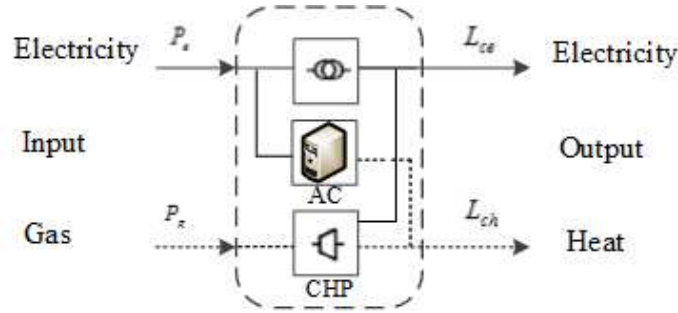
175 exchange power between the CHP and energy networks $P_{e, \text{chp}}$ and $P_{g, \text{chp}}$ (electricity and gas)
 176 can be defined as follow:

$$177 \quad \begin{cases} P_{e, \text{chp}}^{\min} \leq P_{e, \text{chp}} \leq P_{e, \text{chp}}^{\max} \\ P_{g, \text{chp}}^{\min} \leq P_{g, \text{chp}} \leq P_{g, \text{chp}}^{\max} \end{cases} \quad (8)$$

178 where $P_{e, \text{chp}}^{\min}$, $P_{e, \text{chp}}^{\max}$, $P_{g, \text{chp}}^{\min}$, $P_{g, \text{chp}}^{\max}$ can be obtained from Eq. (11) and Eq. (12).

179 3.1.3. Energy hub model

180 The CHP systems include three operating modes, following the electric load mode, following
 181 the thermal load mode, and following hybrid thermal-electric load mode [27]. In this paper, the
 182 EHub model is utilized to describe the CHP system under following hybrid thermal-electric load
 183 mode incorporating different energy system interactions and component constraints.



184
185 Fig. 2 EHub model topology

186 The EHub model in this paper is shown in Fig. 2, which is composed of the power transformer,
 187 microturbine and air-conditioning. The input energy consists of electricity and gas, the output
 188 energy consists of electricity and thermal energy. The energy conversion process can be
 189 described as

$$190 \quad \begin{bmatrix} L_{ce} \\ L_{ch} \end{bmatrix} = \underbrace{\begin{bmatrix} \nu_e & \eta_{ge}^{\text{CHP}} \\ (1-\nu_e)*\eta^{\text{AC}} & \eta_{gh}^{\text{CHP}} \end{bmatrix}}_{C(\nu_e)} \begin{bmatrix} P_e \\ P_g \end{bmatrix} \quad (9)$$

191 where η_{ge}^{CHP} and η_{gh}^{CHP} are the conversion efficiency of gas into electricity and thermal energy
 192 through the CHP respectively; η^{AC} is heat/cold energy conversion rate of the air-conditioner;
 193 P_e and P_g are the power exchanges between EHub and the electricity/gas network; L_{ce} and L_{ch}

194 are the electric and thermal loads provided by EHub. The partition coefficient is used in this
 195 paper, $0 \leq \nu_e \leq 1$, and $\nu_e P_e$ represents the electric power that supplies the electric loads and
 196 $(1 - \nu_e) P_e$ represents the supply of electric power to the air-conditioner.

197 In the CHP systems, the power generation should be equal to the electric load while the
 198 thermal generation can be more than the thermal load by shedding the extra thermal energy.
 199 This gives the equality and inequality constraints for the EHub output power L_{ce} , L_{ch} and the
 200 required power L_e , L_h , as illustrated in Eq. (10).

$$201 \quad \begin{cases} L_e = L_{ce} \\ L_h \leq L_{ch} \end{cases} \quad (10)$$

202 Considering component capacities, the boundaries for the power exchanges between the CHP
 203 systems and the ICES illustrated in Eq. (9) can be expressed as

$$204 \quad (\text{Electricity}) \begin{cases} P_{e, \text{chp}}^{\min} = L_e - P_{\text{mt}}^{\max} \\ P_{e, \text{chp}}^{\max} = L_e + P_{\text{ac}}^{\max} / \eta_{\text{ac}} \end{cases} \quad (11)$$

$$205 \quad (\text{Gas}) \begin{cases} P_{g, \text{chp}}^{\min} = 0 \\ P_{g, \text{chp}}^{\max} = P_{\text{mt}}^{\max} / \eta_{\text{ge}}^{\text{chp}} \end{cases} \quad (12)$$

206 3.1.4. Solving algorithm

207 From the electric power flow model, the gas flow model, and the EHub model, it is known
 208 that there are complex nonlinear relationships between variables in the ICES. Solving the
 209 models as a whole requires high memory requirement and may suffer from the slow convergence
 210 problem. It is difficult to solve the optimization problem using analytical methods. Thus, a
 211 heuristic algorithm, namely particle swarm optimization (PSO) method [28], is used. Denote a
 212 particle position $x_i = [x_{i1}, x_{i2}, \dots, x_{id}]$ and its corresponding flight velocity $v_i = [v_{i1}, v_{i2}, \dots, v_{id}]$
 213 in a d-dimensional search space.

$$214 \quad v_{id}^{t+1} = \omega^t v_{id}^t + c_1 * r_1 * (\text{pbest}_{id}^t - x_{id}^t) + c_2 * r_2 * (\text{gbest}_d - x_{id}^t) \quad (13)$$

$$215 \quad x_{id}^{t+1} = x_{id}^t + v_{id}^{t+1}, i = 1, 2, \dots, n, d = 1, 2, \dots, m \quad (14)$$

216 where n is the number of particles in a group; m is the number members in a particle; t is the
 217 particle generation; ω^t is the inertia weight factor; c_1 and c_2 are acceleration constants; r_1 and r_2
 218 are uniformly distributed random numbers in $[0,1]$; v_i^t is velocity of particle i at iteration t ,
 219 $V_d^{\min} \leq v_{id}^t \leq V_d^{\max}$; x_i^t is current position of particle i at iteration t , $X_d^{\min} \leq x_{id}^t \leq X_d^{\max}$; $pbest_{id}$
 220 represents the recorded individual best position of particle i ; $gbest_d$ represents the recorded
 221 global best position.

222 In this paper, an IOPF method is proposed based on the PSO algorithm as illustrated in Fig.
 223 3, and the algorithm and procedures are summarized as follows:

224
 225 Step 1) (EHub initialization): Compute EHub control variables P_e , P_g , and ε_e according to the
 226 thermal and electric loads in the EHub.

227 Step 2) (Electric power and gas network initialization): Calculate the three-phase power flow
 228 and gas flow separately, and obtain lower and upper bound information for the hybrid gas and
 229 electricity network.

230 Step 3) (PSO initialization): Set the time counter $t_0 = 0$. Initialize randomly the individuals of
 231 the population based on the limit of the EHub (10)-(12). The initial individuals must be feasible
 232 candidate solutions that satisfy the operating constraints.

233 Step 4) (Time update): Update the time counter $t = t + 1$.

234 Step 5) (Hybrid gas and electric power flow computation): Solve gas and electric power flow,
 235 and obtain ICES tie-line power and gas consumptions.

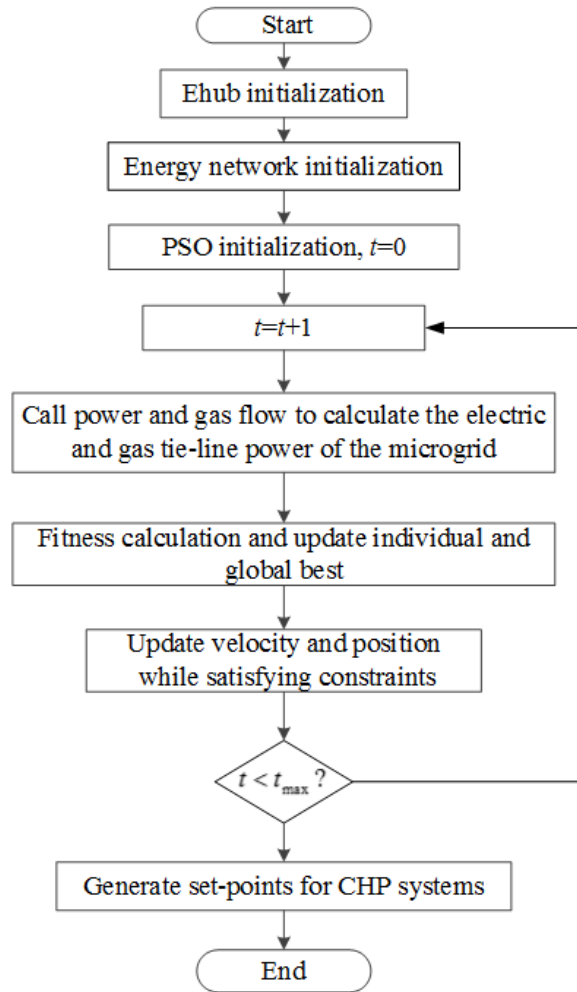
236 Step 6) (Fitness calculation): Calculate the fitness of each individual in the population.

237 Step 7): Update individual best position and global best position.

238 Step 8): Update the velocity and position while satisfying constraints (3)-(8) and (10)-(12).

239 Step 9) (Stop criteria): If the number of iterations reaches the maximum t_{\max} , then go to Step
 240 10). Otherwise, go to Step 5).

241 Step 10): The individual that generates the latest global best position is the optimal solution
 242 with the minimum operating cost.



243

244

Fig. 3 Flowchart of the IOPF for the ICES.

245 3.2. Three-phase demand response dispatch

246 Various DR resources can be flexible to provide the needed fast-response services for
 247 scheduling of the ICES. Considering the three-phase unbalanced load and single-phase DGs in
 248 an ICES, a three-phase DR dispatch method is used in this paper to utilize the DR resources in
 249 different phases and at different locations. The existence of line-pack allows natural gas network
 250 to ehandle short-term gas load fluctuations. Thus, DRs are only used to smooth the electric tie-
 251 line power variations. Considering that DR resources are often distributed in different phases
 252 and locations, a three-phase DR dispatch algorithm is developed. Three-phase electric power

253 systems are considered in this study with the emphasis on single-phase DGs coupled with
 254 unbalanced load.

255 3.2.1. Time series model for thermostatically controlled loads

256 In this paper, heating, ventilating, and air conditioning (HVAC) is studied as thermostatically
 257 controlled loads and a simplified space heating model [29] is used to describe its behaviours.¹
 258 Aggregated HVAC loads are utilized as DR resource units in the three-phase dispatch process.
 259 When the HVAC is turned on or switched off, the room temperature T_{room}^t at time t can be
 260 described by

$$261 \begin{cases} T_{\text{room}}^{t+1} = T_o^{t+1} + QR - (T_o^{t+1} + QR - T_{\text{room}}^t)e^{-\Delta t/RC} & \text{the HVAC is ON} \\ T_{\text{room}}^{t+1} = T_o^{t+1} - (T_o^{t+1} - T_{\text{room}}^t)e^{-\Delta t/RC} & \text{the HVAC is OFF} \end{cases} \quad (15)$$

262 where T_{room}^t represents the room temperature at time t ($^{\circ}\text{C}$); C represents the equivalent heat
 263 capacity ($\text{J}/^{\circ}\text{C}$); R represents the equivalent thermal resistance ($^{\circ}\text{C}/\text{W}$); Q represents the
 264 equivalent heat rate (W); Δt represents the time step (1 minute); and T_o represents the ambient
 265 temperature ($^{\circ}\text{C}$).

266 The DR units in each phase are prioritized in order based on their room temperatures to
 267 generate temperature priority lists (shown in Fig. 4). The upward and down regulations of the
 268 DRs can be expressed based on the ON/OFF status of HVAC temperature priority lists as
 269 described in Eq. (16) and Eq. (17).

$$270 \begin{cases} P_{\text{DR},a,i}^{\text{up}} = \sum_{j=1}^{m_a} P_{\text{rated},j}^i \\ P_{\text{DR},b,i}^{\text{up}} = \sum_{j=1}^{m_b} P_{\text{rated},j}^i \\ P_{\text{DR},c,i}^{\text{up}} = \sum_{j=1}^{m_c} P_{\text{rated},j}^i \end{cases} \quad (16)$$

¹ For practical application, more complex model and normalization method can be used for the time priority list method.

271

$$\begin{cases} P_{DR,a,i}^{down} = \sum_{j=m_a+1}^{N_{DR,a}} P_{rated,i}^j \\ P_{DR,b,i}^{down} = \sum_{j=m_b+1}^{N_{DR,b}} P_{rated,i}^j \\ P_{DR,c,i}^{down} = \sum_{j=m_c+1}^{N_{DR,c}} P_{rated,i}^j \end{cases} \quad (17)$$

272

where m is the number of DR units that are “OFF”; $P_{DR,a,i}^{up}, P_{DR,b,i}^{up}, P_{DR,c,i}^{up}$ and $P_{DR,a,i}^{down}, P_{DR,b,i}^{down}, P_{DR,c,i}^{down}$

273

are the upward and down regulations for group i ; $P_{rated,i}$ is the average rated power of HVACs in

274

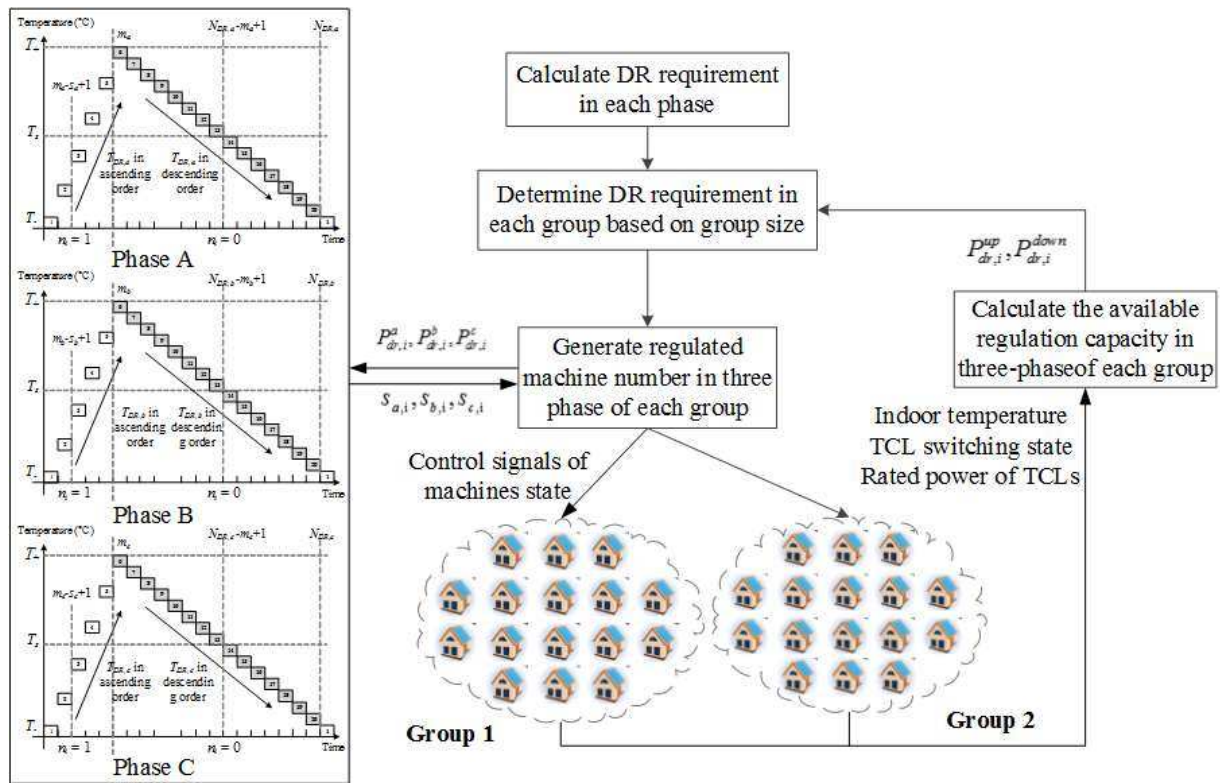
group i ; $m_{a,i}, m_{b,i}, m_{c,i}$ are the numbers of HVACs in group i that are “OFF” for the three

275

phases; $N_{DR,a,i}, N_{DR,b,i}, N_{DR,c,i}$ are the numbers of controllable HVACs in group i for the three

276

phases.



277

278

Fig. 4 Flowchart of the three-phase DR.

279 3.2.2. Objectives

280 Due to the compressibility of natural gas, the gas demand fluctuation can be compensated by
 281 the line-pack in the gas network. Therefore, the control objective in the ultra-short period is to
 282 smooth the tie-line power for the electric power networks as follows

$$\begin{cases}
 P_{DR,a} = \sum_{i=1}^{N_{CHP}} \Delta L_{E,a,i} - \sum_{i=1}^{N_{PV,a}} \Delta P_{PV,a,i} \\
 P_{DR,b} = \sum_{i=1}^{N_{CHP}} \Delta L_{E,b,i} - \sum_{i=1}^{N_{PV,b}} \Delta P_{PV,b,i} \\
 P_{DR,c} = \sum_{i=1}^{N_{CHP}} \Delta L_{E,c,i} - \sum_{i=1}^{N_{PV,c}} \Delta P_{PV,c,i}
 \end{cases} \quad (18)$$

284 where N_{CHP} is the number of CHP systems; $N_{PV,a}$, $N_{PV,b}$, $N_{PV,c}$ are the numbers of photovoltaics
 285 (PVs) plugged in three-phase; $\Delta L_{E,a,i}$, $\Delta L_{E,b,i}$, $\Delta L_{E,c,i}$ are the short-term three-phase electrical
 286 load forecasting errors of CHP system i ; $\Delta P_{PV,a,i}$, $\Delta P_{PV,b,i}$, $\Delta P_{PV,c,i}$ are the short-term forecasting
 287 errors of the i th PV three-phase output.

288 3.2.3. Algorithm implementation

289 A group-based DR approach is proposed to alleviate the communication burden caused by
 290 the unified scheduling for huge volumes of DR resources. This also covers the utilization of the
 291 DR resources in different phases and at different locations. DR units are split into groups based
 292 on their distributed locations, and three phase dispatch is implemented based on the DR
 293 requirement in three-phase for each group respectively. At the client level, the available
 294 regulation capacity of each group in three phases is calculated based on the ON/OFF status of
 295 HVACs for the master level. In the master level, DR requirements (Eq. (18)) in each group are
 296 calculated based on the group size as shown in Eq. (19).

$$\left\{ \begin{array}{l}
 P_{DR,a,i} = \frac{P_{DR,a} C_{DR,a,i}}{\sum_{i=1}^{N_g} C_{DR,a,i}} \\
 P_{DR,b,i} = \frac{P_{DR,b} C_{DR,b,i}}{\sum_{i=1}^{N_g} C_{DR,b,i}} \\
 P_{DR,c,i} = \frac{P_{DR,c} C_{DR,c,i}}{\sum_{i=1}^{N_g} C_{DR,c,i}}
 \end{array} \right. \quad (19)$$

297 where N_g is the number of DR groups; $C_{DR,a,i}$, $C_{DR,b,i}$, $C_{DR,c,i}$ are the capacities of controllable

298 HVACs in group i for three phases; $C_{DR,a,i} = \sum_{j=1}^{N_{DR,a,i}} P_{rated,i}$, $C_{DR,b,i} = \sum_{j=1}^{N_{DR,b,i}} P_{rated,i}$, $C_{DR,c,i} = \sum_{j=1}^{N_{DR,c,i}} P_{rated,i}$;

300 $P_{rated,i}$ is the average rated power of HVAC units in group i .

301 The feasibility domain is defined by the DR regulation limits

$$\left\{ \begin{array}{l}
 P_{DR,a,i}^{lower} \leq P_{DR,a,i} \leq P_{DR,a,i}^{upper} \\
 P_{DR,b,i}^{lower} \leq P_{DR,b,i} \leq P_{DR,b,i}^{upper} \\
 P_{DR,c,i}^{lower} \leq P_{DR,c,i} \leq P_{DR,c,i}^{upper}
 \end{array} \right. \quad (20)$$

303 where $P_{DR,a,i}$, $P_{DR,b,i}$, $P_{DR,c,i}$ are the DR power at each phase in group i .

304 The adjusted power in each group, $P_{DR,a,i}$, $P_{DR,b,i}$, $P_{DR,c,i}$ are converted to the number of HVAC

305 units required to be regulated $s_{a,i}$, $s_{b,i}$, $s_{c,i}$ as illustrated by

$$\left\{ \begin{array}{l}
 s_{a,i} = \left\lfloor \frac{P_{DR,a,i}}{P_{rated,i}} \right\rfloor \\
 s_{b,i} = \left\lfloor \frac{P_{DR,b,i}}{P_{rated,i}} \right\rfloor \\
 s_{c,i} = \left\lfloor \frac{P_{DR,c,i}}{P_{rated,i}} \right\rfloor
 \end{array} \right. \quad (21)$$

307 3.3. Implementation of the hierarchical management algorithm

308 As discussed in Section 2, the hierarchical energy system consists of day-ahead scheduling

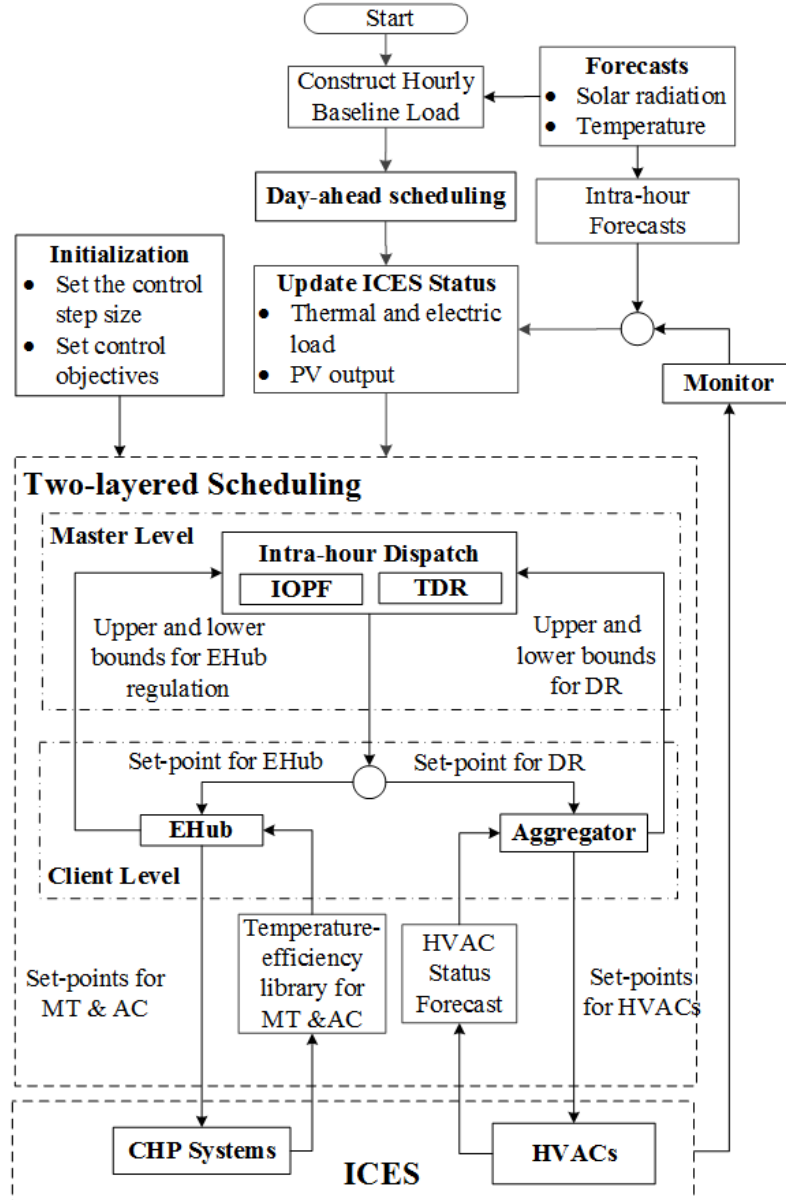
309 and intra-hour adjustment. In the day-ahead scheduling, initial set-points are generated for

310 energy hub outputs. A master-client structure is embedded in the intra-hour adjustment system

311 to manage the CHP and the DR in two different time scales. In order to handle the system

312 unbalance and single phase DG variation, the loads in three phases are managed synthetically.

313 The proposed algorithm is introduced as follows (see Fig. 5):



314

315

Fig. 5 Flowchart of the hierarchical management for the ICES.

316

317

318

319

Step 1) (ICES initialization): Set the control objectives and scheduling periods for CHP systems and DR resources according to the actual operation status of the ICES and the client demand. As mentioned earlier, the control objective is set to minimize the operation cost for day-ahead scheduling (shown in Eq. (1)); the control objective is to follow the electric and gas

320 tie-line power set-points for short term intra-day scheduling (shown in Eq. (2)); while for ultra-
321 short term intra-day scheduling (shown in Eq. (18)), the control objective is to smooth the tie-
322 line power for the electricity networks.

323 Step 2) (Day-ahead scheduling): Given the load and generation forecasting results (hourly
324 forecasting), day-ahead scheduling results (24 hour power and gas dispatch signal for the clients)
325 are obtained by the IOPF program.

326 Step 3) (Update ICES status): Update ICES status (DG output/ short term and ultra-short term
327 load forecast results) based on load and generation short term forecast results (intra-hour
328 forecast) and measured data.

329 Step 4) (Intra-day scheduling, including dispatch of CHP systems and three-phase DR
330 resources): A two-layered scheduling method is proposed to balance time-varying energy
331 demand and supply while to meet the requirement of interrelated constraints between multiple
332 energy systems.

333 At the master level, the main dispatch tasks are:

- 334 • For CHP systems, the IOPF is called to generate set-points for CHP systems to follow
335 the electric and gas tie-line power based on the day-ahead electric and gas tie-line power
336 scheduling results and DGs short term forecast results;
- 337 • For the DR resources, generate power regulation command for each phase (described in
338 Eq. (18)) based on the three-phase electrical load and DGs ultra-short term forecast
339 results; Then, determine DR requirements in each group based on group size (described
340 in Eq. (19)) and the regulation limits (described in Eq. (19)) could be taken into account
341 in the regulation.

342 At the client level, the main dispatch tasks are:

- 343 • For CHP systems, on one hand, generate set-points for components of CHP systems
344 based on the EHub model; One the other hand, calculate the feasibility domain of the
345 power exchange between the CHP and energy networks $P_{e, \text{chp}}$ and $P_{g, \text{chp}}$ (electricity and
346 gas) based on the Eq. (11) and (12) and upload the upper and lower bounds for CHP
347 systems to the master level;
- 348 • For DR resources, on one hand, calculate the feasibility domain of the DR regulation

349 based on Eq. (16) and (17) and upload the upward and down regulations to the master
 350 level; On the other hand, the regulated power in each group, $P_{DR,a,i}$, $P_{DR,b,i}$, $P_{DR,c,i}$ are
 351 converted to the number of HVAC units required to be regulated² $S_{a,i}$, $S_{b,i}$, $S_{c,i}$ as illustrated
 352 in Eq. (21).

353 In this paper, the electrical system is an unbalanced three-phase power system. The software
 354 of Open Distribution System Simulator (OpenDSS) [30] is used to solve the electric power flow.
 355 The proposed algorithm has been implemented based on the OpenDSS simulation engine that
 356 calculates three-phase electric power flow and Microsoft Visual C++ that performs the gas flow,
 357 EHub, PSO, and three-phase DR algorithm.

358 4. Case studies

359 The test system in Fig. 6 is used to investigate the proposed hierarchical management system.
 360 Based on the solar forecast results as shown in Fig. 7, the output of the PV panels and the CHP
 361 component efficiency can be obtained. To highlight the effectiveness of the proposed method,
 362 only load variations connected to the CHP systems 1 and 2 are considered in this paper. The
 363 ICES investigated in this paper includes the following main components:

- 364 • IEEE 37-bus radial distribution feeder [31], and the bus voltage is subject to the
 365 constraint $0.9 \leq V \leq 1.1$;
- 366 • A 4-node natural gas network, and the gas network data is shown in Table 1. The gas
 367 network used in this paper was initially designed for line-pack studies. Thus, wider
 368 pipelines are utilized in the network³. The upper and lower limits of the compression
 369 ratio are $k_{cp}^{\min} = 1.2$ and $k_{cp}^{\min} = 1.8$ respectively; the upper and lower limits of natural gas
 370 pipeline pressure are $p^{\min} = 0.2$ and $p^{\max} = 1.3$, respectively.

²The regulation method of controllable loads (take HVAC as example) is based on the commonly used assumption in inconsistent literatures, etc. the system state at next time step could be predicted accurately based on the system state in the current time step, and the prediction technique for HVAC would be further studied in the future research.

³ In order to ensure the gas network pressure level above a certain range, gas companies requires customer who use gas-fired generators to have gas storage devices. However, due to the security requirements, customers usually don't have enough room for gas storage. An alternative way is to install wider pipelines with line-pack as storage.

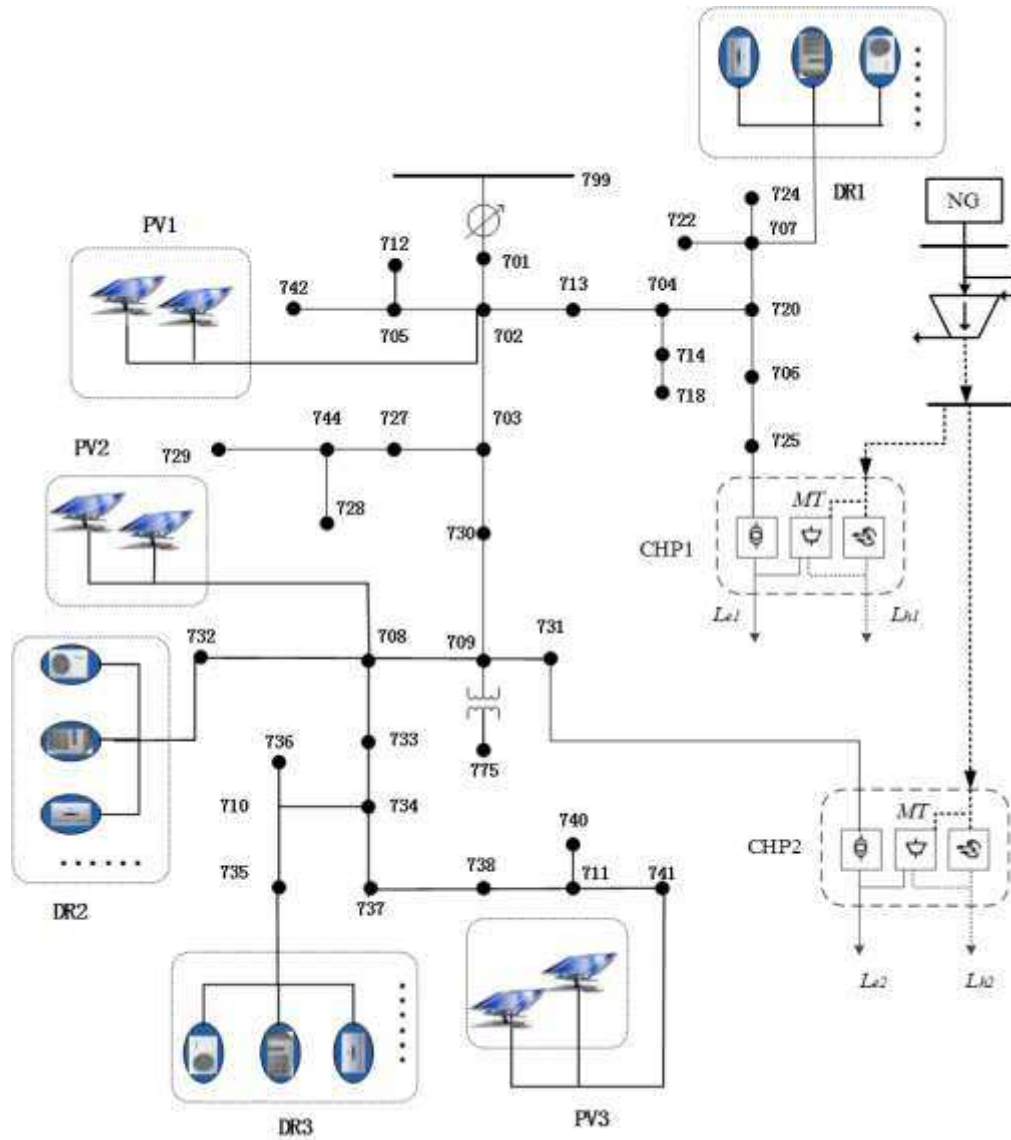


Fig. 6 Scheme diagram of the ICES case.

Table 1.
Natural gas network parameters

| Pipe number | Start node | End node | Pipeline Diameter(mm) | Pipeline Length(m) |
|-------------|------------|----------|-----------------------|--------------------|
| 1 | 1 | 2 | 900 | 500 |
| 2 | 2 | 3 | 900 | 500 |
| 3 | 2 | 4 | 900 | 500 |

371

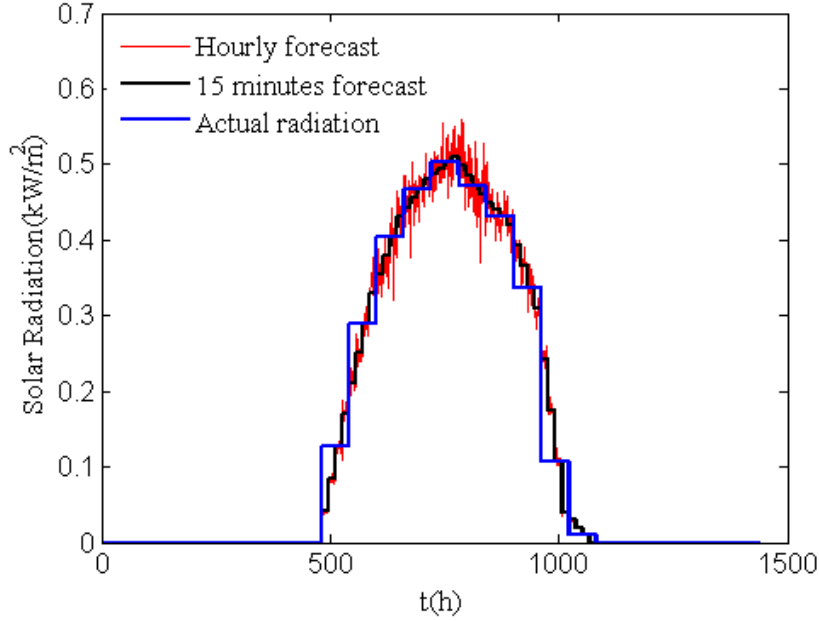
372

373

374

375

- 376 • Three PV panels are connected to the electric power network via bus 702, 708, and 741.
 377 The rated power of the three PV panels are 1000kW, 60kW (A-phase) and 2000kW. The
 378 actual and forecasted radiation levels are shown in Fig. 7;



379

Fig. 7 Solar radiation data.

380

- 381 • Two EHubs, consisting of transformers, microturbines, and air-conditioners, are
 382 connected to bus 725, 731 in the electric power network and node 003, 004 in the gas
 383 network. The EHub data is presented in Table 2;

384

Table 2.

385

EHub Component Capacity

| | EHub number | Value (kW) | EHub number | Value (kW) |
|----|-------------|------------|-------------|------------|
| MT | 1 | 300 | 2 | 300 |
| AC | 1 | 100 | 2 | 100 |

386

- 387 • Three groups of HVAC units at bus 707, 732, and 735 are used for demand response.
 388 Considering that not all customers would like to participate in the DR program, only a
 389 certain number of HVAC units are incorporated in the DR, as shown in Table. 3. The
 390 rated power of HVACs is 1 kW with a dead band of 4 °C. Customer thermostat settings,
 391 T_{set} , are set to be 23 °C. The mean values of C, R, and Q are set to 3599.3 J/°C, 0.1208

392 °C/W, and 400 W respectively. The parameters C, R, and Q are randomized to create
 393 load diversity.

394 Table 3.
 395 HVAC number in each phase of the three groups.

| Group number | Bus number | Phase A | Phase B | Phase C |
|--------------|------------|---------|---------|---------|
| 1 | 707 | 210 | 210 | 210 |
| 2 | 732 | 270 | 270 | 270 |
| 3 | 735 | 150 | 150 | 150 |

396
 397 The electricity and gas from distribution networks are included in the overall simulation. The
 398 energy price used in this paper is taken from PG&E [32]. By providing renewable generation
 399 smoothing, the local energy supplier can obtain some profits from the utility. In this paper, this
 400 profit is not considered in the economic interests of the local energy supplier. Since the DR is
 401 only used for small adjustment, a fixed subsidy can be used that will not affect the operating
 402 cost optimization. More complex market model and pricing mechanism will be investigated in
 403 future work.

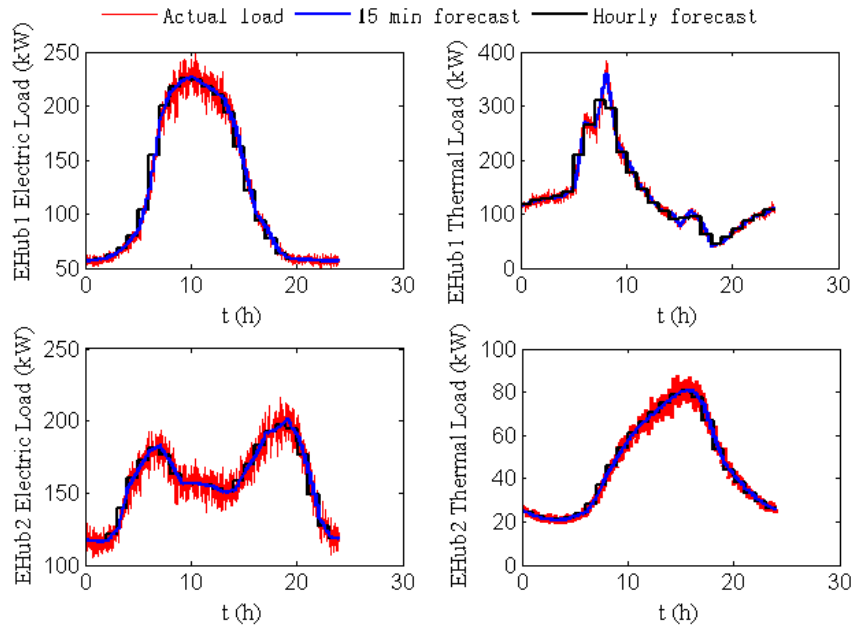
404 5. Results and discussion

405 5.1. Day-ahead scheduling

406 The 24 hour profile of the load is presented in Fig. 8 with hourly forecast and short term (15
 407 minutes) forecast results, together with realistic load data. The CHP power input boundaries are
 408 calculated using the EHub model.

409 At the master level in the hierarchical scheme, the feasibility domain of the power exchange
 410 between the CHP and the energy networks $P_{e, \text{chp}}$ and $P_{g, \text{chp}}$ (electricity and gas) are calculated,
 411 and a 24 hour power and gas dispatch signals are generated for the clients in order to minimize
 412 the operating cost by utilizing the IOPF tool. The energy price and the operating cost are shown
 413 in Fig. 9. The 24 hour power and gas dispatch results to minimize the operating cost are shown
 414 as the red solid line and the 24 hour power and gas dispatch results to minimize the electrical
 415 power loss are shown by the blue dotted lines in Fig. 10. The comparison of the two dispatch
 416 results suggests that the operation cost of the ICES can be reduced significantly through the

417 optimal dispatch. The 24 hour day-ahead scheduling EHub (EHub1 and EHub2) electric/gas
 418 regulation signals and the feasibility domain of the exchange power between the CHP and
 419 energy networks are depicted in Fig. 11.

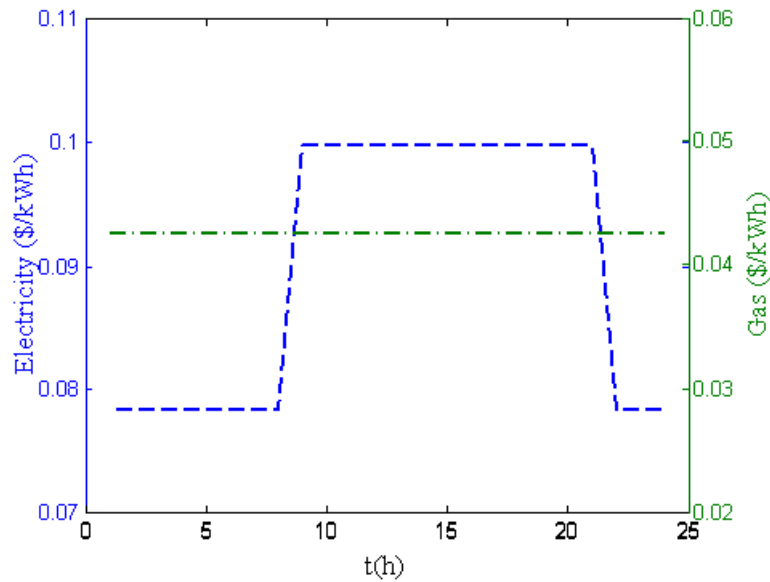


420

421

Fig. 8 CHP system loads.

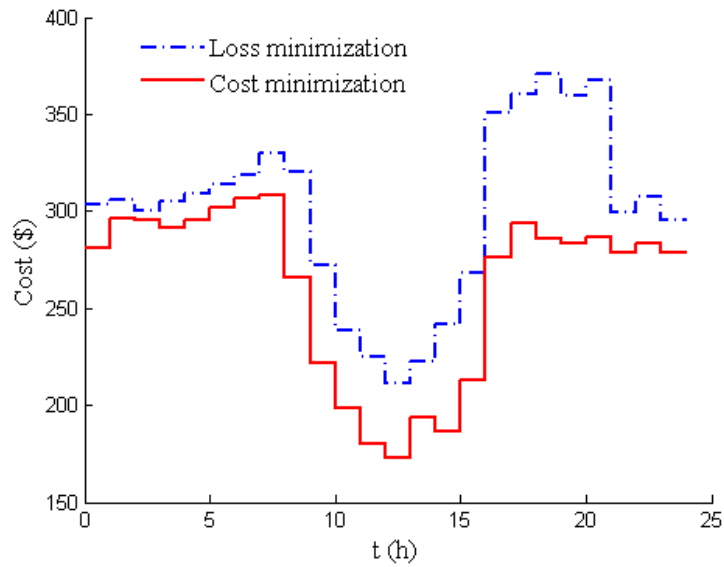
422



423

424

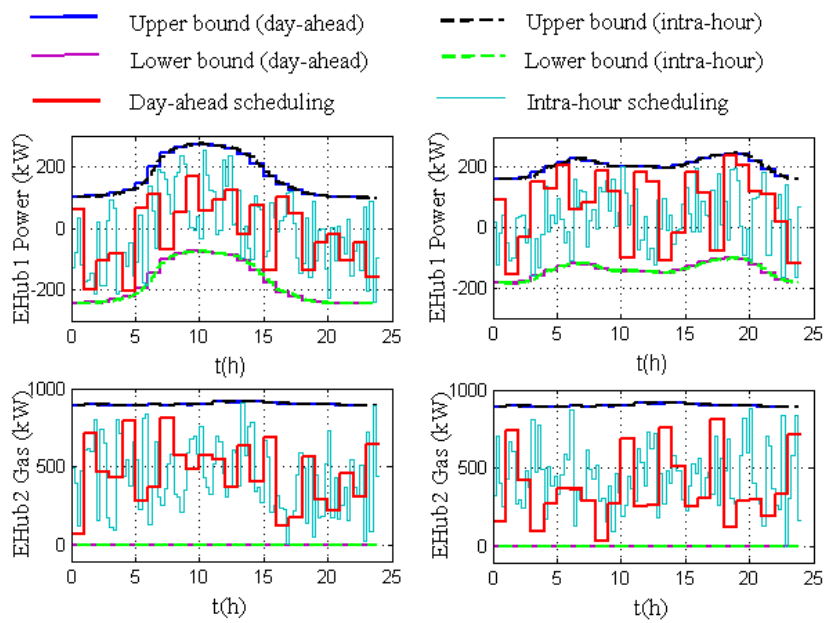
Fig. 9 Energy price.



425

426

Fig. 10 ICES operating cost comparison under different objectives.



427

428

Fig. 11 Set-points and bounds for CHP systems.

429 5.2. Intra-hour scheduling

430 5.2.1. CHP regulation test

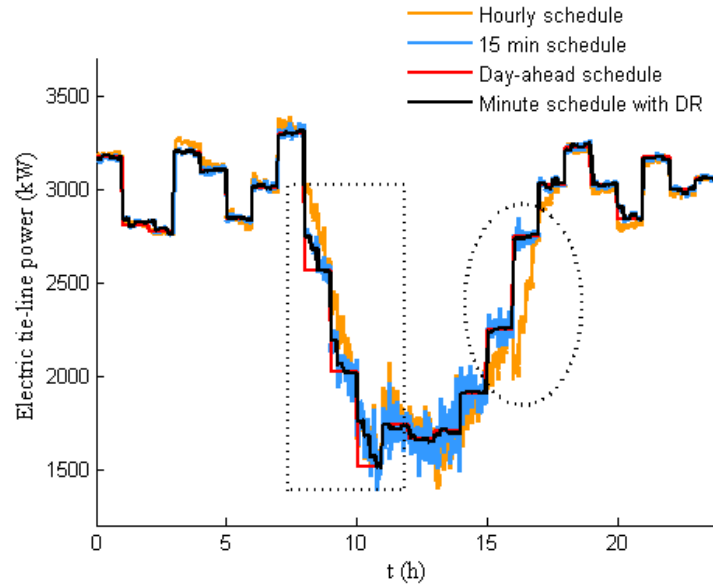
431 Considering that microturbines and air-conditioners are not suitable for frequent adjustment,
432 the control period for the CHP is set to be 15 minutes. Based on the set-point obtained from the
433 master level and the short-term load forecast signals as depicted by the black and blue line in
434 Fig. 8, the CHP input is adjusted within the limits. Since the gas pipeline network can mitigate
435 the flow fluctuations to some extent due to the gas storage characteristic of the pipeline network,
436 the IOPF program is called to track the electric tie-line power mainly in intra-hour scheduling.
437 Therefore, a relatively large value for ω_e in Eq. (2) is taken, and gas tie-line power tracking is
438 considered under the natural gas pipeline network constraints.

439 At the client level, the upper and lower power regulation boundaries for EHub1 and EHub2
440 (represented by the black and green dotted lines in Fig. 11) are calculated, based on the load and
441 DGs short term forecast results. The boundaries for the CHP systems to the master level are also
442 calculated for short term dispatch. At the master level, the exchange power between the CHP
443 and electric power/gas networks are regulated to track the electric and gas tie-line power set-
444 points obtained in day-ahead scheduling for smoothing the tie-power fluctuations caused by the
445 day-ahead forecast errors. The electric/gas regulation signals of EHub1 and EHub2 are
446 described by the cyan solid lines in Fig. 11, which suggests that the CHP can effectively respond
447 to the intra-hour scheduling commands and the regulation power of EHub1 and EHub2 are
448 within the feasibility domain to guarantee the customer comfort level.

449 Two scenarios have been developed to verify the effectiveness of the proposed hierarchical
450 scheduling method for smoothing the electric/gas tie-line power fluctuations as follows:

451 **Scenario I:** Intra-hour scheduling of the ICES based on the day-ahead scheduling results.
452 The day-ahead scheduling discussed in section 5.1 is shown by the red solid line in Fig. 12, and
453 the intra-hour scheduling results without short term dispatch of the CHP systems are shown by
454 the yellow solid line in Fig. 12. When there is electric power /gas energy shortage caused by
455 day-ahead forecasting errors in the ICES, all the energy shortage would be supplied by electrical
456 power (electric loads are supplied by the electric power network and the thermal loads are
457 supplied by the ACs in CHP systems) without the short term dispatch of CHP systems, and the

458 electric/gas tie-line power fluctuations will mainly be reflected in the electric tie-line power
 459 fluctuations, which is shown by the yellow solid line in Fig. 12.



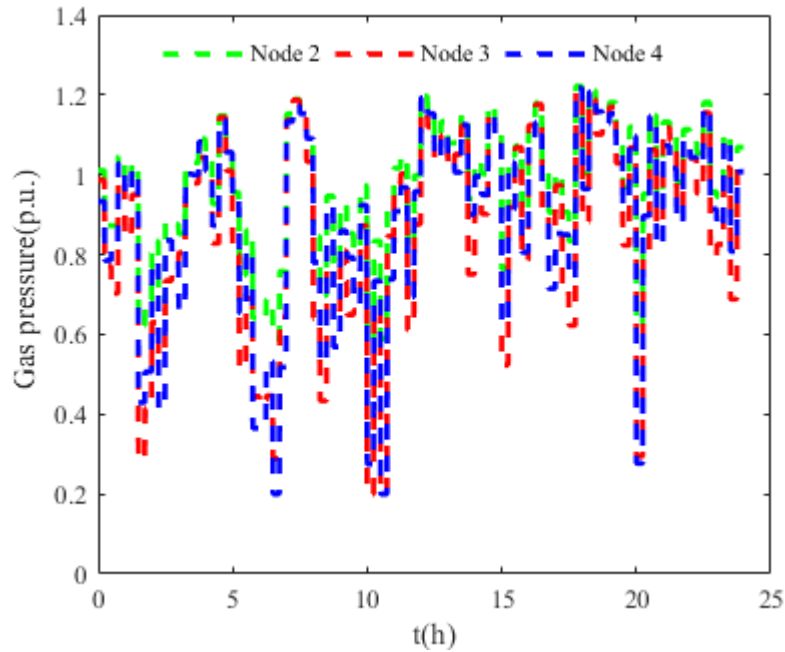
460

461

Fig. 12 ICES electric tie-line power.

462 **Scenario II:** Further conduction of 15 minute ahead scheduling based on the scheduling
 463 results taken from Scenario I. The exchange power between the CHP and electric/gas networks
 464 is regulated to track the electric and gas tie-line power set-points obtained from the day-ahead
 465 scheduling for smoothing the tie-line power fluctuations. The scheduling results in Scenario II
 466 are shown by the blue solid line in Fig. 12.

467 The comparison of scheduling results in Scenario I and Scenario II (shown in Fig. 12.)
 468 suggests that the electric tie-line power fluctuations of the ICES can be reduced to some extent
 469 using the short term dispatch of CHP systems. It is worth noting that electric tie-line power
 470 fluctuations still exist after the short term dispatch of the CHP systems due to the 15 minutes
 471 scheduling period for the CHP system. With the 15 minute scheduling results, the natural gas
 472 network pressure is shown in Fig. 13. It can be seen that the obtained gas network pressure are
 473 under the permissible range considering gas flow constraints. As previously mentioned, the
 474 operator tends to use more gas when the gas price is low. If gas flow constraints are not
 475 considered, the scheduling objective cannot be achieved. Moreover, the large amount of gas
 476 consumption will affect the gas pressure level of other loads.



477

478

Fig. 13 Natural gas network pressure.

479

5.2.2. Three-phase DR scheduling test

480

481

482

483

484

As previously mentioned, the DR resources are used to balance the load and DG forecasting mismatch in an ultra-short control period to guarantee the customer comfort level. As another type of clients, HVAC groups are used to compensate the ultra-short term (1 minute) forecasting mismatch. The initial room temperature and ON/OFF status are set by randomizing each HVAC for 24 hours.

485

486

487

488

Scenario III is developed to verify the effectiveness of the proposed three-phase DR dispatch method. The dispatch based on the scheduling results from Scenario II is conducted to further smooth the electric tie-line power fluctuations. The specific scheduling procedure is introduced as follows:

489

490

491

492

493

At the master level, the power regulation commands are generated for DR in each phase (described in Eq. (18)) based on the three-phase electrical load and DG ultra-short term forecast results. Then, the DR requirement in each group is determined based on the group size (described in Eq. (19)). The DR required power and HVACs temperature of Phase A in the three groups after DR dispatching are shown in Fig. 14.

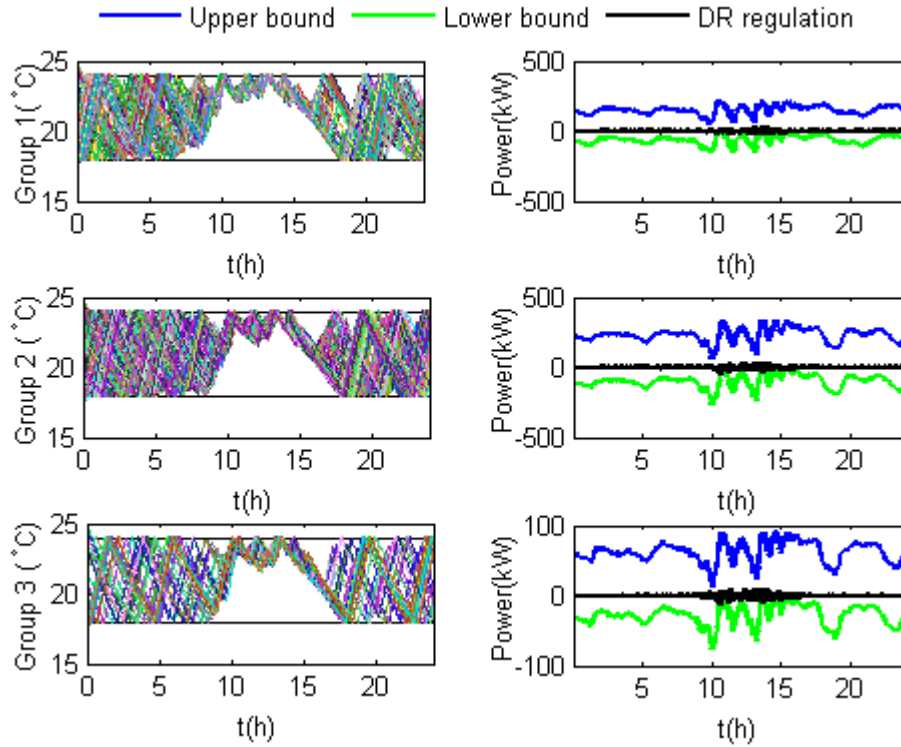


Fig. 14 DR of Phase A in the three groups.

494

495

496

497

498

499

500

501

502

503

504

505

506

507

508

509

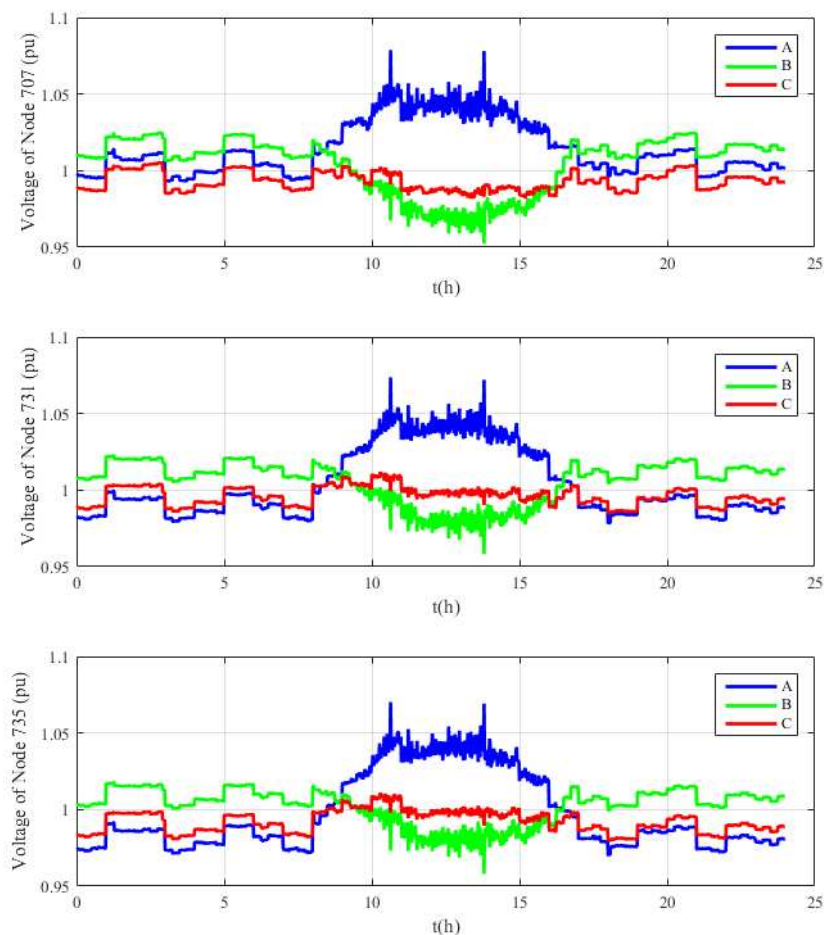
510

At the client level, the feasibility domain of the DR regulation is calculated first based on the ON/OFF status of HVACs in each group, and the boundaries for the DR regulation are generated by the client as illustrated in the green and blue area of Fig. 14. The boundaries are uploaded to the master for the short period dispatch.

The simulation results reveal that the DR signals (the black line in Fig. 14) are dispatched to the three groups within the limits. All the HVACs are operated in the dead band. It is worth noting that PV outputs increase in 10-15 hours leading to the increase of the electric tie-line power fluctuations, and the DR required power increases accordingly while the boundaries for the DR regulation are narrowed in the three groups. The relative voltage at each node of the HVACs is shown in Fig. 15.

A comparison of the scheduling results in Scenario III (black solid line in Fig. 12), Scenario I (yellow solid line in Fig. 12) and Scenario II (blue solid line in Fig. 12) suggests that the tie-power fluctuations are well smoothed by the DR. A small number of fluctuations shown in the red lines are due to the DR dispatch signals reaching the boundaries of the HVACs. In addition

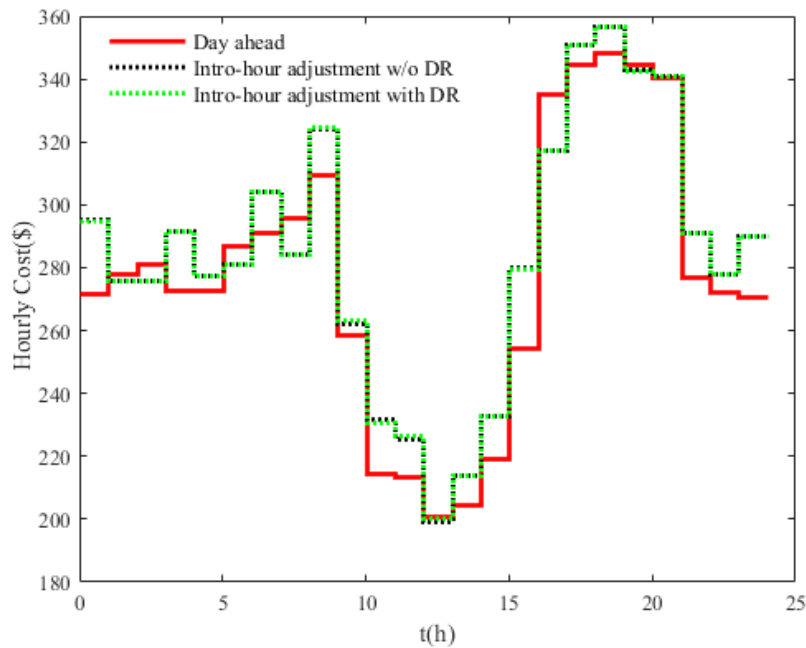
511 to the tie-line power, the operating cost in the three scenarios are shown in Fig. 16. It can be
 512 seen that although there are some mismatch between the set points and the real operating points
 513 due to forecast errors, the operating cost is close to the day-ahead schedule. In the meanwhile,
 514 the tie-line power fluctuation is significantly reduced as depicted in Fig. 12. Because the DR is
 515 not charged in this paper, the intra-hour dispatch with and without DR has almost the same
 516 operating cost unless the DR reach its boundaries (see the dashed green line and black line). By
 517 providing controllable tie-line response, the energy service provider can earn some profits from
 518 utilities and pay customers some money for the DR. Considering the positive effect of the DR
 519 on smoothing the tie-line power flow, it is possible for energy service providers to negotiate
 520 with both utilities and customers to obtain more profits and reducing operating costs.



521

522

Fig. 15 Three-phase voltage of the aggregated loads.



523

524

Fig. 16 Operating cost comparison between the three scenarios.

525

6. Conclusion

526 This paper designed a hierarchical management system for a community area by scheduling
 527 the CHP and demand response. It allows the operators to coordinate the interrelated power, gas
 528 and heat systems, taking three-phase electric power system characteristics into account. With
 529 the integrated optimal power flow method, optimal operating plan can be generated for CHP in
 530 the day-ahead scheduling. For intra-hour scheduling, a two-layered approach is designed to
 531 follow the day-ahead operating plan, taking into account the uncertainties associated with
 532 renewable generations and loads. To incorporate various device characteristics, CHPs and
 533 demand response are coordinated at two different time scales. At the master level, CHP systems
 534 are dispatched to follow the electric and gas tie-line power set-points within a short-term. A
 535 three-phase demand response method is further presented to smooth the electric tie-line power
 536 fluctuations by managing loads and DGs from various locations and at different phases within
 537 an ultra-short term. At the client level, the operating boundaries for the CHP and the DR are

538 generated and transmitted to the upper layer. The set-points from the upper level are then
539 converted to control signals for each unit.

540 The developed methodology is applied to a simulated community energy system obtained
541 from a modified IEEE 37-node system. Numerical results have shown that the proposed
542 scheduling method can effectively reduce the operating cost while smooth the tie-power power
543 fluctuations. It is also shown that the amount of data traffic will be significantly reduced as only
544 the operating boundary information is transmitted. The proposed method can also be used to
545 meet other requirements for the integrated community energy system, such as minimizing the
546 energy loss and emissions.

547 **Acknowledgements**

548 This work was financially supported by the National Science Foundation of China (No.
549 51377117 and No. 61273040), the National High-tech R&D Program of China (863 Program
550 with No. 2015AA050403), the National Social Science Foundation of China (No. 12&ZD208),
551 the Distinguished Visiting Fellowship Scheme of the Royal Academy of Engineering
552 (DVF1415/2/59), and Engineering and Physical Sciences Research Council (EPSRC) under
553 Grant No. EP/L001063/1.

554 **Reference**

- [1] S. Dirks, and M. Keeling. A vision of smarter cities: How cities can lead the way into a prosperous and sustainable future. IBM Institute for Business Value. June 2009.
- [2] G. Mendes, C. Ioakimidis, and P. Ferrão. On the planning and analysis of Integrated Community Energy Systems: A review and survey of available tools. *Renew Sust Energ Rev* 2011; 15(9): 4836-4854.
- [3] G. Chicco, P. Mancarella. Distributed multi-generation: a comprehensive view. *Renew Sust Energ Rev* 2009; 13: 535-551.
- [4] C. Marnay, G. Venkataramanan, M. Stadler, A. S. Siddiqui, R. Firestone, and B. Chandran. Optimal technology selection and operation of commercial-building microgrids. *Power Syst IEEE Trans* 2008; 23(3): 975-982.

-
- [5] C. Marnay, G. Venkataramanan, M. Stadler, A. Siddiqui, R. Firestone, B. Chandran, Optimal technology selection and operation of microgrids in commercial buildings, in: Power Engineering Society General Meeting. Proc IEEE 2007: 1–7.
- [6] R. Lasseter, A. Akhil, C. Marnay, J. Stephens, J. Dagle, R. Guttromson, etc. The CERTS microgrid concept. White paper for Transmission Reliability Program, Office of Power Technologies, US Department of Energy, 2002.
- [7] H. Lund, A. N. Andersen, P. A. Østergaard, B. V. Mathiesen, and D. Connolly. From electricity smart grids to smart energy systems—a market operation based approach and understanding. *Energy* 2012; 42(1): 96-102.
- [8] X. Ma, Y. Wang, J. Qin. Generic model of a community-based microgrid integrating wind turbines, photovoltaics and CHP generations. *Appl Energy* 2013; 112: 1475-1482.
- [9] X. Liu, J. Wu, N. Jenkins, A. Bagdanavicius. Combined analysis of electricity and heat networks. *Appl Energy*, <http://dx.doi.org/10.1016/j.apenergy.2015.01.102>.
- [10] M. Geidl, G. Andersson, Optimal power flow of multiple energy carriers. *Power Syst IEEE Trans* 2007; 22(1): 145–155.
- [11] A. Shabanpour-Haghighi, A. R. Seifi. Simultaneous integrated optimal energy flow of electricity, gas, and heat. *Energy Convers Manage* 2015; 101: 579-591.
- [12] A. Shabanpour-Haghighi, A. R. Seifi. Multi-objective operation management of a multi-carrier energy system. *Energy* 88, 2015, 430-442.
- [13] G. C. Heffner, C. A. Goldman, M. M. Moezzi. Innovative approaches to verifying demand response of water heater load control. *Power Del IEEE Trans* 2006; 21(1): 388–397.
- [14] H. Jia, Y. Qi, Y. Mu. Frequency response of autonomous microgrid based on family-friendly controllable loads. *Sci China Ser E Technol Sci* 2013; 56(3): 693-702.
- [15] B. Dupont, K. Dietrich, C. De Jonghe, A. Ramos, R. Belmans. Impact of residential demand response on power system operation: A Belgian case study. *Appl Energy* 2014; 122: 1-10.
- [16] Wu, Hongyu, Mohammad Shahidehpour, Ahmed Alabdulwahab, and Abdullah Abusorrah. Demand response exchange in the stochastic day-ahead scheduling with variable renewable generation. *Sustain Energy IEEE Trans* 2015; 6(2): 516-525.
- [17] X. Wang, A. Palazoglu, N. H. El-Farra, Operational optimization and demand response of hybrid renewable energy systems. *Appl Energy* 2015; 143(1): 324-335.

-
- [18] Y. Kitapbayev, J. Moriarty, P. Mancarella. Stochastic control and real options valuation of thermal storage-enabled demand response from flexible district energy systems. *Appl Energy* 2015; 137: 823-831.
- [19] A. Navarro-Espinosa, P. Mancarella. Probabilistic modeling and assessment of the impact of electric heat pumps on low voltage distribution networks. *Appl Energy* 2014; 127: 249-266.
- [20] O. Palizban, K. Kauhaniemi, and J. M. Guerrero. Microgrids in active network management-Part I: Hierarchical control, energy storage, virtual power plants, and market participation. *Renew Sust Energ Rev* 2014; 36: 428-439.
- [21] X. Wu, X. Wang, C. Qu. A Hierarchical Framework for Generation Scheduling of Microgrids. *Power Del IEEE Trans* 2014; 29(6): 2448-2457.
- [22] X. Xu, H. Jia, D. Wang, D. C. Yu, and H. Chiang. Hierarchical energy management system for multi-source multi-product microgrids. *Renew Energy* 2015; 78: 621-630.
- [23] M. Mao; P. Jin; N. D. Hatziargyriou, Chang L. Multi agent-Based Hybrid Energy Management System for Microgrids. *Sustain Energy IEEE Trans* 2014; 5(3): 938-946.
- [24] B. Jiang, Y. Fei. Dynamic residential demand response and distributed generation management in smart microgrid with hierarchical agents. *Energy Procedia* 2011; 12: 76-90.
- [25] M. Z. Kamh, R. Iravani. Unbalanced model and power-flow analysis of microgrids and active distribution systems. *Power Del IEEE Trans* 2010; 25(4): 2851-2858.
- [26] E. Shashi Menon. *Gas pipeline hydraulics*. CRC Press, 2005.
- [27] Y. Ruan, Q. Liu, W. Zhou, R. Firestone, W. Gao, T. Watanabe. Optimal option of distributed generation technologies for various commercial buildings. *Appl Energy* 2009; 86(9): 1641–1653.
- [28] Z. L. Gaing. Particle swarm optimization to solving the economic dispatch considering the generator constraints. *Power Syst IEEE Trans* 2003; 18(3), 1187-1195.
- [29] N. Lu. An evaluation of the HVAC load potential for providing load balancing service. *Smart Grid IEEE Trans* 2012; 3(3): 1263-1270.
- [30] R. C. Dugan, Reference guide: The open distribution system simulator (opends), Electric Power Research Institute, Inc.
- [31] W. H. Kersting. "Radial distribution test feeders." *Power Engineering Society Winter Meeting, IEEE* 2001; 2.
- [32] Pacific Gas&Electrc. Tariffs. A-10 TOU, 200-500kW, <http://www.pge.com/tariffs/electric.shtml>